Published in final edited form as:
*J Control Release*. 2011 October 30; 155(2): 119–127. doi:10.1016/j.jconrel.2011.06.009.

# ADVANCED MOLECULAR DESIGN OF BIOPOLYMERS FOR TRANSMUCOSAL AND INTRACELLULAR DELIVERY OF CHEMOTHERAPEUTIC AGENTS AND BIOLOGICAL THERAPEUTICS

**William B. Liechty**[1], **Mary Caldorera-Moore**[1,2], **Margaret A. Phillips**[2], **Cody Schoener**[1], and **Nicholas A. Peppas**[1,2,3,*]

[1]Department of Chemical Engineering, The University of Texas at Austin, Austin, TX 78712, USA

[2]Department of Biomedical Engineering, The University of Texas at Austin, Austin, TX 78712, USA

[3]Division of Pharmaceutics, The University of Texas at Austin, Austin, TX 78712, USA

## Abstract

Hydrogels have been instrumental in the development of polymeric systems for controlled release of therapeutic agents. These materials are attractive for transmucosal and intracellular drug delivery because of their facile synthesis, inherent biocompatibility, tunable physicochemical properties, and capacity to respond to various physiological stimuli. In this contribution, we outline a multifaceted hydrogel-based approach for expanding the range of therapeutics in oral formulations from classical small-molecule drugs to include proteins, chemotherapeutics, and nucleic acids. Through judicious materials selection and careful design of copolymer composition and molecular architecture, we can engineer systems capable of responding to distinct physiological cues, with tunable physicochemical properties that are optimized to load, protect, and deliver valuable macromolecular payloads to their intended site of action. These hydrogel carriers, including complexation hydrogels, tethered hydrogels, interpenetrating networks, nanoscale hydrogels, and hydrogels with decorated structures are investigated for their ability respond to changes in pH, to load and release insulin and fluorescein, and remain non-toxic to Caco-2 cells. Our results suggest these novel hydrogel networks have great potential for controlled delivery of proteins, chemotherapeutics, and nucleic acids.

### Keywords

Responsive Hydrogels; Oral Delivery; Protein Delivery; Nanoscale Hydrogels; Interpenetrating Network

## I. INTRODUCTION

The development of molecularly engineered biomaterials has been motivated by the challenges of controlled transmucosal and intracellular delivery of both hydrophobic drugs and macromolecular biotherapeutics, such as proteins and nucleic acids. Intelligent materials that can sense and respond to physiological and biological cues demonstrate promise in helping engineers and scientists overcome the significant challenges of achieving efficient

*To whom correspondence should be addressed. Phone: 512-471-6644 Fax: 512-471-8227 peppas@che.utexas.edu.

oral administration of fragile therapeutics [1]. For these applications, researchers in our laboratory have developed a new class of crosslinked hydrogels composed of poly(ethylene glycol) (PEG)-containing grafted copolymers of acrylic acid (AA), methacrylic acid (MAA) or 2-diethylaminoethyl methacrylate (DEAEMA), containing functional compounds such as carbohydrate-binding proteins [2], polysaccharides, and targeting ligands [3]. In our recent work, we have shown that biomacromolecular delivery from these hydrogels can be controlled by their three-dimensional network structure as well as the conditions of the surrounding environment as these systems exhibit reversible hydrogen bonding and interpolymer complexation/decomplexation [4, 5].

Promising new studies indicate that this class of hydrogel carriers, including complexation hydrogels, tethered hydrogels, nanoscale hydrogels, and hydrogels with decorated structures, can be used for delivery of hydrophobic drugs or biomacromolecules such as proteins and small interfering RNA (siRNA) [6, 7].

A molecular understanding of how these hydrogels interact with and respond to biological environments is fundamental to continued development of transmucosal and intracellular drug delivery systems. For example, understanding the mucoadhesive behavior of PEG-containing carriers in contact with the intestinal mucosa is of utmost importance in local protein delivery, especially in the upper small intestine [8]. An important contributor to successful transmucosal delivery is adhesion to the intestinal mucosa through the presence of molecular adhesion promoters such as PEG chains grafted to crosslinked networks, lectins attached to hydrogels [2], and novel hydrogel structures decorated with carbohydrates [9].

In recent years, our laboratory has demonstrated great success in polymer-mediated delivery of fragile biomacromolecules such as insulin [10], calcitonin [11], and interferon β [12]. We now turn our attention to expanding the suite of fragile therapeutics available via oral administration. Through rational molecular design of novel polysaccharide-modified complexation hydrogels, we aim to improve bioavailability of therapeutic proteins by enhanced biophysical interaction with intestinal mucosa. Increased understanding of transport phenomena in tumor environments and the behavior of biomaterials in physiological environments are paramount to our goal of developing highly efficient oral delivery systems for chemotherapeutic drugs. New therapeutic modalities, such as RNA interference, have given researchers a host of new tools with which to treat previously intractable diseases. To this end, we are exploring nanoscale hydrogel carriers as siRNA delivery vehicles to disease targets along the GI tract [9, 13–18].

### I.1 Tethered Carriers and Protein Delivery

One particular structural modification of interest is the decoration of micro- and nanoparticle surfaces with chains containing specific flexibility and functional groups. Specifically, our laboratory has studied PEG-tethered complexation hydrogels for controlled oral delivery of proteins. A central aim of our work has been protection of the protein bioactivity and to ensure therapeutic bioavailability. The seminal work of Lowman et al. [10, 19–22] demonstrated that three-dimensional network structure could be used to control diffusion of proteins in gastric fluids. Promising studies from other groups [23] showed that erodible polyanhydride polymers displayed strong interactions with the mucosa of the gastrointestinal tract, suggesting that these microparticles could be used for delivery of insulin and plasmid DNA. Subsequent studies by our laboratory have focused on tailoring the structures of complexation hydrogels to address the major challenge to oral delivery of protein drugs–low bioavailability. Low bioavailability is attributed [24] to protein drugs' chemical instability in the gastrointestinal (GI) tract, susceptibility to proteolysis, and reduced ability to traverse biological barriers due to size [25].

One unique attribute of poly(methacrylic acid)-grafted-poly(ethylene glycol) (P(MAA-g-EG)) complexation hydrogels is their ability to protect protein drugs from enzymatic and chemical degradation upon exposure to intestinal fluids [26]. Several studies in our laboratory have shown that the structure of P(MAA-g-EG) hydrogels in acidic conditions as well as chemical composition contribute to this phenomenon. At low pH, the formation of physical crosslinks due to hydrogen bond formation between the poly(methacrylic acid) (PMAA) backbone and the PEG tethers limits diffusion into and out of the gel. Using insulin-loaded P(MAA-g-EG) microparticles, Wood et al. demonstrated limited release (< 10%) of insulin during a 60 minute incubation in simulated gastric conditions [2]. Following a step change in pH from pH 3.2 to pH 7.0, 80% of the insulin was released within 30 minutes. The theoretical distance these adjacent cross links, or mesh size, $\zeta$, can be calculated by well-known techniques [27]. We have also shown that PMAA can bind $Ca^{2+}$ thereby inhibiting $Ca^{2+}$-dependent proteases [26, 28]. For insulin and hemoglobin, Lehr and coworkers reported inhibition of proteolytic degradation in the presence of adhesive poly(acrylic acid)-based hydrogels [29, 30].

Bioadhesive drug delivery systems capable of concentrating release at the absorption site are one strategy for improving protein drug absorption and increasing bioavailability [18]. The residence time of the carrier at the site of absorption, the upper small intestine, is an important contributing factor to the bioavailability of orally administered protein drug delivery systems. If the residence time of the carrier is extended in the upper small intestine, there is a longer window for protein drug absorption as well as higher concentration gradients at the absorption site. Our design of bioadhesive drug delivery systems relies on a fundamental understanding of how hydrogels interact with mucosal membranes and biological tissues. Serra et al. [8, 31, 32] have carried out molecular and structural studies to analyze the nature of the adhesive interactions. Thomas et al. [17, 33, 34] have used these studies to develop a new class of PEG-containing adhesive carriers. Moreover, to take advantage of mucoadhesion due to chain interpenetration, our laboratory has proposed adding adhesion promoters composed of long, linear polymer tethers extending from the hydrogel surface [18, 31, 35]. A number of studies have demonstrated hydrogels with PEG tethers are mucoadhesive and have increased residence time in the upper small intestine [8, 32, 34, 36]. More recently, we have focused on biomolecules to promote adhesion, with an effort to develop a mechanistic understanding of molecular adhesion. The primary goal of bioadhesive controlled drug delivery is to localize a delivery device within the body to enhance the drug absorption process in a site-specific manner. Wheat germ agglutinin-functionalized P(MAA-g-EG) gels [2] have shown promising results in vitro and in vivo. In this work, we have modified P(MAA-g-EG) hydrogels with neutral polysaccharide tethers of dextran and pullulan to form P(MAA-g-EG-Dextran) and P(MAA-g-EG-Pullulan) hydrogels.

### I.2 Nanoscale hydrogels in drug delivery

Several recent efforts have explored the utility of responsive nanoscale hydrogel carriers in drug delivery [3, 37–39], demonstrating release of biological therapeutics such as insulin and imaging agents such as gold. Nanoscale hydrogels are increasingly attractive as drug delivery agents owing to their facile manufacture, tunable physicochemical characteristics, and repeatable release. Furthermore, their covalent crosslinking endows them with mechanical integrity not available in their self-assembled counterparts.

**Applications in Cancer Treatment—**Significant advancements have been made in our fundamental understanding of cancer; but unfortunately these developments have not yet been fully translated into effective clinical treatments of cancer [40]. A major reason is our inability to administer therapeutic agents selectively to the targeted sites while avoiding

adverse effects on healthy tissue. Current therapeutic strategies for most cancers involve a combination of surgical resection, radiation therapy, and chemotherapy. These therapies are associated with significant morbidity and mortality primarily due to their non-specific effects on “normal” cells. The increase in efficacy of a therapeutic formulation is directly correlated to its ability to selectively target diseased tissue, overcome biological barriers, and intelligently respond to the disease environment to release therapeutic agents.

Nanotechnology coupled with advanced cancer biology offers great potential for addressing these challenges [41]. In recent years, outstanding progress has been made using nanovectors, liposomes, and polymer-mediated delivery strategies to increase localized delivery by (a) targeting drugs to tumor cells and (b) increasing serum residence time [42, 43]. Although these strategies have reduced systemic toxicity, significant improvements on delivery strategies are still necessary to increase patient quality of life and reduce chemotherapy-related side effects.

The development of oral delivery systems for chemotherapeutic agents has recently been explored in order to minimize the side effects of the intravenous administration, increase the effectiveness of the drug, and improve the patient’s quality of life [44–46]. Recent studies have demonstrated that orally-delivered chemotherapeutic agents were effective relative to conventional intravenous administration [47–51]. However, low bioavailability due to poor absorption, degradation of drugs in the acidic environment of the stomach, and gastric enzymes in the leaky upper part of the small intestine must be circumvented for oral administration of chemotherapeutic agents to be an effective delivery strategy. In addition, an effective delivery strategy must protect the GI tract from the potential toxicity of these chemotherapeutic agents.

An anionic pH-responsive hydrogel is well-suited to overcome these barriers due to its ability to release drug in the upper small intestine in response to increased pH. Researchers in our laboratory have produced pH-responsive hydrogels, P(MAA-g-PEG), that have demonstrated great potential as an oral drug delivery system of hydrophilic cancer and protein based drugs [52–55]. Many popular chemotherapy drugs currently used are hydrophobic, which limits their ability to interact favorably with hydrophilic pH-responsive hydrogels for oral delivery. In this research, we are focusing on developing pH-responsive polymers with hydrophobic moieties that will enable efficient loading and responsive release of hydrophobic drugs like doxorubicin and fluorouracil.

Oral hydrogel chemotherapy delivery systems require hydrophobic components to favorably interact with the chemotherapeutic. Our laboratory has taken two approaches: 1) incorporation of hydrophobic monomers into our grafted hydrogel network and 2) interpenetrating polymer networks (IPNs) comprised of hydrophilic and hydrophobic networks. For the first approach, our laboratory has focused on nanoscale gels of the P(MAA-g-EG) copolymers with added hydrophobic monomer *t*-butyl methacrylate polymerized into the hydrogel network (P(MAA-co-*t*-BMA-g-PEG)).

In addition, our laboratory has developed sequential interpenetrating polymer networks (IPNs) which are characterized by interwoven or entangled individual polymer networks. IPNs with networks of opposing or complementing properties with a hydrogel network (P(MAA-g-EG)) and an interpenetrating hydrophobic network (poly(butyl acrylate)), have been developed in our laboratory for oral chemotherapy delivery [39, 56].

**Applications in nucleic acid delivery—**Additional efforts in our lab aim to develop nanogel-based platform technologies for delivery of siRNA. The landmark discovery of RNA interference (RNAi) in 1998 has sparked a massive research effort in all fields of

biological science and redefined our understanding of gene regulation mechanisms [57]. Theoretically, RNAi mediated by siRNA could be used as a powerful and versatile treatment modality to treat nearly any disease resulting from aberrant gene expression. Owing to its remarkable potency and reversible therapeutic effect, siRNA holds extraordinary promise as a new biological therapeutic. As with many biotherapeutics, efficient delivery has been implicated as the major hurdle to its widespread clinical application [58]. Though much effort has been directed toward synthetic polymer carriers for siRNA, there remains a paucity of data on the development of oral delivery systems. The goal of our work is to develop a novel hydrogel platform for siRNA delivery; a synthetic polymer carrier capable of delivering siRNA to disease targets along the gastrointestinal tract. Amine-containing methacrylates, such as 2-(diethylaminoethyl) methacrylate (DEAMA) [59] and 2-(dimethylaminoethyl) methacrylate (DMAEMA) [60], are attractive foundations for polymeric nucleic acid-delivery systems because of their ability to form cooperative electrostatic interactions with polyanionic siRNA. We have previously developed DEAEMA-based polycationic nanogels [3, 37] and are currently investigating their utility as highly-efficient siRNA delivery vectors. However, a critical aspect of intracellular delivery systems is a mechanism for elimination or degradation. Disulfide linkers can be cleaved by the reductive tripeptide glutathione; present at intracellular concentrations of 1 – 11 mM [61]. By incorporating these linkers into polycationic nanogels, we can impart degradability to the network while retaining their mechanical integrity and pH-responsive behavior.

## II. EXPERIMENTAL SECTION

### II. 1. Polymerization of P(MAA-g-EG) Hydrogels

P(MAA-g-EG) films were prepared by a free radical UV-initiated polymerization. Briefly, a 1:1 (by weight) solution of ethanol and water was prepared. To the solvent, an equal mass of monomers was added. The monomers consisted of methacrylic acid (MAA, Sigma Aldrich) and poly(ethylene glycol) monomethyl ether monomethacrylate (PEGMA, Polysciences Inc.) with an average molecular weight of 1000 Da combined in a ratio of 1 mol MAA to 1 mol EG. The crosslinker poly(ethylene glycol) dimethacrylate (PEGDMA, Polysciences Inc.) with an average molecular weight of 400 Da was added to comprise a desired percent of the total monomers, the percent crosslinker. The initiator, Irgacure 184 (Ciba Geigy), was added to be 0.1 wt% of the total monomers. The solution was sonicated for 20 minutes then purged with nitrogen for 30 minutes inside a glove box, which was purged for the same amount of time. The solution was then placed in a mold consisting of two glass slides and a Teflon spacer. The polymerization was started upon exposure to ultraviolet (UV) light with an intensity of 16–17 $mW/cm^2$ for 30 minutes. The resulting film was then washed in ultrapure water for 7 days and the water was exchanged twice daily to remove any unreacted components. Films were dried in a vacuum oven and then crushed and sieved to form microparticles 90–120 μm in diameter.

### II. 2. Polymerization of P(MAA-g-EG-co-Polysaccharide) Hydrogels

To form P(MAA-g-EG-co-Dextran) and P(MAA-g-EG-Pullulan) gels, methacrylate groups were added to dextran (average number molecular weight 6 kDa or 100 kDa; Sigma Aldrich, St. Louis, MO) or pullulan (average number molecular weight 75 kDa; Sigma Aldrich, St. Louis, MO) as reported previously [62]. The methacrylated polysaccharides were incorporated into P(MAA-g-EG) hydrogel films using a UV-initiated free radical solution polymerization. In order to solubilize dextran with the other monomers, modifications were made to the P(MAA-g-EG) synthesis. The solvent was 73% 0.1 N sodium hydroxide and 27% ethanol solution. MAA was first solubilized in sodium hydroxide, followed by Dextran-methacylate or Pullulan-methacrylate, PEGMMA, PEGDMA, ethanol, and then Irgacure 184. The solution was sonicated for 20 minutes or until the reactants were fully

dissolved. The polymerization followed the same procedure outlined for P(MAA-g-EG) gels.

### II. 3. Polymerization of Nanoscale Hydrogels

Nanoscale hydrogels were synthesized via UV-initiated free radical photoemulsion polymerization according to previous reports from our laboratory [3, 37]. Briefly, 2-(diethylamino) ethyl methacrylate (DEAEMA, Sigma-Aldrich), 2-(*tert*-butylamino)ethyl methacrylate (*t*-BAEMA, Polysciences, Inc.), *tert*-butylamino methacrylate (*t*-BMA, Sigma-Aldrich), and tetra(ethylene glycol) dimethacrylate (TEGDMA, Sigma-Aldrich) were passed through a column of basic alumina powder to remove inhibitor prior to use. Methacrylic acid (MAA, Aldrich Chemical Co.) was vacuum distilled at 54°C/25 mmHg to remove the inhibitor, and poly(ethylene glycol) methyl ether methacrylate (PEGMMA), $M_n \sim 2080$, (Sigma-Aldrich) was used as received. Bis(2-methacryloyloxyethyl) disulfide (SSXL) was synthesized according to a previous report [63]. Crosslinker and monomer were added to an aqueous solution of 5 wt% PEGMMA, Irgacure 2959 (Ciba Geigy) at 0.5 wt% of total monomer, 4 mg $mL^{-1}$ Brij-30 and ionic surfactant myristrimethylammonium bromide (MyTAB) or sodium dodecyl sulfate (SDS), depending on the ionic nature of the monomer. The mixture was emulsified using a Misonix Ultrasonicator (Misonix, Inc.). The emulsion was purged with nitrogen gas and exposed to a UV source for 2.5 hr with constant stirring. Surfactants and unreacted monomers were removed by repeatedly inducing polymer-ionomer collapse, separating particles by centrifugation, and resuspending in 0.5 N HCl for cationic particles or 0.5 N NaOH for anionic particles. Polymer particles were dialyzed against $ddH_20$ for 7 days with the water changed twice daily.

### II.4. Synthesis of P(MAA-g-EG)/P(BA) IPNs

The hydrophobic-hydrophilic IPNs were prepared by sequential UV-initiated free radical polymerization. First, hydrophilic P(MAA-g-EG) networks were synthesized as described in section II.1 and crosslinked with TEGDMA rather than PEGDMA. The resulting film was washed for 7 days to remove unreacted components and dried in vacuo. To form the second network, dried P(MAA-g-EG) films were incubated overnight in a solution of butyl acrylate, TEGDMA, Irgacure 184, and a solvent consisting of various ratios of ethanol and water. The solutions were then purged with nitrogen. The films were placed on an open-faced glass plate and exposed to UV light allowing polymerization of the second network. The resulting IPN was washed to remove unreacted components and dried in vacuo. Three unique IPNs were synthesized by varying the ethanol to water ratio of the soaking solution: 80/20 IPN, 75/25 IPN, and 70/30 IPN.

### II. 5 Characterization

**Equilibrium Swelling Studies—**Equilibrium swelling studies were performed on dry polymer disks of P(MAA-g-EG-co-Dextran 6,000), P(MAA-g-EG-co-Dextran 100,000), and P(MAA-g-EG-Pullulan 75,000). The initial mass of the gels was recorded. Gels were then incubated in 50 mL 10 mM 3,3-dimethylglutaric acid (DMGA) buffers with different pHs (pH = 3.2 to 7.6) at 37°C and constant ionic strength for 24 hours. The final mass of the swollen gels was used to calculate the equilibrium mass swelling ratio.

**Contact Angle Measurements—**Surface analysis was carried out on a Rame-Hart Goniometer (Model No. 100) and analyzed with DROPimage software. Using HPLC water, a 5 μL sessile drop was placed on 3 random locations on an IPN or P(MAA-g-EG) disc. Images were captured at time equal 0 sec and 120 sec and the angle formed between the disc surface and water droplet were analyzed to determine extent of hydrophobicity.

**Dynamic Light Scattering (DLS)—**The hydrodynamic diameter in aqueous suspension of the polymer networks was measured using a Malvern Zetasizer NanoZS (Malvern Instruments Corp.) operating with a 633 nm laser source equipped with MPT-2 Autotitrator. DLS measurements of particle size and pH-responsive behavior were conducted by resuspending lyophilized particles in PBS at 0.5 mg $mL^{-1}$. For cationic particles, the suspension pH was adjusted to 10.5 using 1 N NaOH and gradually lowered to pH 3.5 using 1 N HCl. In contrast, the suspension pH for anionic particles was decreased to 4.5 and then gradually increased to pH 9 using 1 N NaOH. Measurements of the z-average particle size were collected at 25°C and pH intervals of 0.5.

**Electrophoretic Light Scattering—**The effective surface ζ-potential of the polymer networks was measured using a Malvern Zetasizer NanoZS (Malvern Instruments Corp.) operating with a 633 nm laser source equipped with MPT-2 Autotitrator. Measurements of ζ-potential as a function of pH were conducted by resuspending lyophilized particles in 5 mM phosphate buffer at 0.5 mg/mL. The suspension pH was adjusted to 10.5 using 1 N NaOH and gradually lowered to pH 3.5 using 1 N HCl. Electrophoretic light scattering measurements of the surface ζ-potential were collected at 25°C with nanogels suspended in 5 mM sodium phosphate.

**Electron Microscopy—**TEM micrographs were collected using a FEI Tecnai Transmission Electron Microscope (80 kV) at magnifications from 16,500× to 160,000×. Lyophilized particles were diluted in $ddH_2O$ and stained with 2% uranyl acetate immediately prior to imaging. Particle volume in the dry state was taken as the cube of mean diameter from TEM images. Particle diameters were calculated from the particle area as determined by an ImageJ particle sizing algorithm. Reported values represent the mean ± standard deviation ($n > 50$). SEM micrographs were collected using a Zeiss Supra 40 VP scanning electron microscope and coated with a 8 nm layer of Pt-Pd immediately prior to imaging.

**Cytocompatibility Studies—***In vitro* cytocompatibility was determined for polycationic and polyanionic nanoscale hydrogel networks using the CellTiter 96 AQueous One Solution Cell Proliferation Assay kit (Promega Corp., Madison, WI) in which the soluble tetrazolium salt [3-[4,5-dimethylthiazol-2-yl]-5-(3-carboxymethoxyphenyl)-2-(4-sulfophenyl)-2H-tetrazolium] (MTS) is reduced to a purple formazan product. The absorbance of the formazan product is proportional to the number of viable cells. Stock solutions of polymer were suspended in PBS and allowed to equilibrate overnight. Caco-2 cells were seeded in 96-well plates at 15,000 cells/well and incubated for 36 hours prior in 200 μL Dulbecco's Modified Eagles Medium supplemented with 100 U $mL^{-1}$ penicillin, 100 μg $mL^{-1}$ streptomycin, and 10% FBS. Media was aspirated and cells were washed 2× with DPBS and incubated in serum-free DMEM for 90 minutes. Following this incubation period, polymer stock solutions at 5× were added to cells for another 90 minutes. Media and polymer were aspirated and replaced with a DMEM/MTS solution. Absorbance at 490 nm was recorded after 4 hours incubation in the DMEM/MTS solution.

### II. 6. Loading and Release Studies

P(MAA-g-EG), P(MAA-g-EG-co-Dextran 6,000), P(MAA-g-EG-co-Dextran 100,000) and P(MAA-dg-EG-Pullulan 75,000) microgels of 90 – 120 μm were loaded with insulin according to published protocol [64]. During the loading process, the initial insulin and final insulin concentration were sampled and measured by aqueous high throughput liquid chromatography (HPLC). The loading efficiencies, the ratio of the mass of insulin loaded to the initial insulin mass, for modified and unmodified P(MAA-g-EG) gels were compared.

Release studies were carried out using a USP 2 dissolution apparatus according to established protocols. Insulin-loaded particles (30 mg) were added to 30 mL of 1X PBS at 37 oC and were stirred with impellers at 100 rpm. Samples of 200 μL were taken at 0, 5, 10, 15, 30, 60, and 120 minutes after the addition of the microparticles, and the concentration of insulin was determined by HPLC. To compare release from different polymers, the ratio of mass of insulin released to the final mass of insulin released was calculated (Figure 1b).

HPLC was performed to determine insulin concentrations using a Waters Alliance HPLC unit equipped with a Symmetry C4 5 μm column. The mobile phase consisted of 70% water with 0.1% trifluoroacetic acid (TFA) and 30% acetonitrile with 0.08% TFA. The column was heated to 40°C. A gradient was run in the reverse direction from 30% to 60% acetonitrile over a 6 minute time period. The sample run time was 10 minutes, and the sample injection volume was 20 μL. Absorbance was measured at 220 nm.

P(MAA-g-EG) and IPN microparticles of 75–500 μm were loaded with fluorescein according to the following procedure: fluorescein was dissolved in 2% (w/w) dimethyl sulfoxide in 1X PBS to a concentration of 0.145 g $mL^{-1}$. To this stock solution dried microparticles were added and allowed to stir 24 hr. After 24 hr, the initial and final fluoroscein concentrations were sampled and measured on a BIO-TEK SynergyHT UV/VIS plate reader to determine amount loaded. Loaded particles were lyophilized for 48 hrs.

Release of fluorescein loaded particles were conducted with two modifications: 10 mg of fluorescein loaded particles were added to 30 mL 1X PBS and sampling was extended to 4 and 6 hr time points. The concentration of fluorescein was determined by UV/VIS plate reader.

## III. RESULTS AND DISCUSSION

In this work, we studied a variety of complexation hydrogels for transmucosal and intracellular delivery of hydrophobic drugs or biomacromolecules. The performance of each drug delivery system was evaluated based on the material properties as it applied to the specific application and drug. For example, the pH-dependent complexation behavior of each of these hydrogels was studied for either oral delivery or intracellular delivery. Hydrogels which undergo a sharp swelling transition at different pHs are highly advantageous for both oral delivery and intracellular delivery. The pH-dependent complexation behavior of P(MAA-g-EG) hydrogels has been well studied in our laboratory. In acidic conditions, physical crosslinks form as a result of interpolymer complexes. Interpolymer complexation is due to hydrogen bonding between pendant MAA along the polymer backbone and etheric oxygen of PEG tethers. In acidic milieu, the mesh size of the network, ξ, the distance between adjacent junctions, formed either by covalent or physical crosslinks, is small. The small mesh size limits diffusion into and out of the hydrogel network. At more neutral conditions, at pHs above the pKa of MAA, deprotonation of pendant MAA results in decomplexation. Decomplexation causes the mesh size to increase as a result of fewer hydrogen bonds, permitting efflux of entrapped macromolecular therapeutics. Macroscopically, complexation behavior results in a sharp swelling transition between the non-swollen and swollen state as a function of pH.

For transmucosal delivery of protein drugs using polysaccharide-modified hydrogels, the effect of large polysaccharides on complexation behavior and drug loading and release was studied. The complexation behavior of P(MAA-g-EG-co-Dextran) and P(MAA-g-EG-co-Pullulan) hydrogels was evaluated by determining the equilibrium mass swelling ratios in buffer over pHs relevant to the gastrointestinal tract. Data shown in Figure 2 demonstrate the hydrogels have pH-dependent complexation behavior and that decomplexation occurs

between a pH of 5 and 6. Swelling transitions in this range are desirable for triggered release in the upper small intestine. Additionally, we observed that hydrogels with the lowest molecular weight dextran (6 kDa) exhibit maximum swelling greater than hydrogels with larger dextran (100 kDa) or pullulan (75 kDa) polysaccharide components at pH 5 – 7.

The ability to load and release protein drugs from P(MAA-g-EG-co-Dextran) and P(MAA-g-EG-co-Pullulan) gels was demonstrated with insulin. As shown in Figure 3, insulin release was more rapid from 53–75 μm diameter microparticles composed of either P(MAA-g-EG-co-Dextran) or P(MAA-g-EG-co-Pullulan) than P(MAA-g-EG) controls. The two formulations with lower molecular weight polysaccharides including the P(MAA-g-EG-co-Dextran 6,000) microgels and the P(MAA-g-EG-co-Pullulan 75,000) controlled release of insulin over the 2 hour release study more effectively than the P(MAA-g-EG-co-Dextran 100,000) which released all of the drug in 20 less than minutes. It is possible that this difference in insulin release rate may be due to polymer-protein interactions, as insulin has been shown to interact more favorably with PEG than with Dextran [65].

To evaluate anionic complexation nanogels with hydrophobic moieties for oral chemotherapeutic delivery applications, we evaluated the material properties including the nanogel size and morphology and the complexation of these hydrogels. Successful synthesis of P(MAA-g-EG) carriers with hydrophobic comonomers P(MAA-co-*t*-BMA-g-PEG) was shown using scanning electron microscopy (SEM) and transmission electron microscopy (TEM). Figure 4 shows the synthesized nanoparticles after purification both before lyophilization (Figure 4a-b) and after lyophilization (Figure 4c-d). As observed in Figure 4, the particle size is affected by post-synthesis steps. Particle diameter is decreased following lyophilization.

DLS was used to study the effects of the hydrophobic comonomer on complexation behavior. It is well known that addition of hydrophobic or hydrophilic comonomers can shift the pKa of the pH- and temperature-dependent swelling [3, 66, 67]. From DLS measurements of lyophilized P(MAA-co-*t*-BMA-g-PEG) particles that were re-hydrated in PBS (Figure 5), an increase in the particle volume is observed with increasing pH above 4.8 which is close to the pKa of MAA. A swelling transition at pH 4.8 indicates that drug release as a result of decomplexation would occur in the upper small intestine.

Characterization and evaluation of the P(MAA-g-EG)/P(BA) IPNs focused on the effect of polymerization conditions on hydrophobicity and drug loading and release. Contact angle measurements were conducted to determine if the ratio of hydrophobic P(BA) network differed between various IPN formulations. Table 1 demonstrates the gradual increase in hydrophobicity across IPN formulations, confirming the hypothesis that P(BA) content increases as a result of the degree of swelling during the second network photopolymerization. By tailoring the polymer chemistry, the resultant physicochemical properties of the IPNs could be tuned to optimize them for chemotherapeutic loading and release.

Evaluation of hydrophobic drug loading and release was investigated using fluorescein, a fluorescent dye with similar hydrophobicity, chemical structure, and molecular weight as chemotherapeutics. IPN microparticles (75–400 μm) were loaded with fluorescein. Table 1 presents the loading efficiencies of IPNs and P(MAA-g-EG). The 75/25 IPN showed a balance of swelling and hydrophobic components to optimize loading levels. The release profiles for the IPNs illustrated over 80% release of contained drug by 2 hr, a time scale relevant to transit through the small intestine.

A panel of polycationic nanoscale hydrogels comprised of a crosslinked core of poly[2-(diethylaminoethyl) methacrylate] surface grafted with poly(ethylene glycol) was

synthesized using photoemulsion polymerization. Polymer composition was varied to determine the effect of crosslinking density and core hydrophobicity on physicochemical properties and drug delivery efficacy. Analysis of TEM micrographs revealed successful formation of nanoscale hydrogel networks. All preparations appear to have a narrow particle size distribution with a mean diameter of approximately 50 nm. Specifically, dry diameters of 51 ± 14 nm for P(DEAEMA-*g*-PEGMMA) (PDET) crosslinked with TEGDMA, 52 ± 16 nm for P(DEAEMA-co-*t*-BAEMA-g-PEGMMA) crosslinked with TEGDMA (PDETBA15), 52 ± 15 nm for P(DEAEMA-co-*t*-BMA-g-PEGMMA) crosslinked with TEGDMA (PDETB20) and 50 ±17 nm for P(DEAEMA-co-*t*-BMA-g-PEGMMA) crosslinked SSXL (PDESSB20) were observed.

Figure 9 illustrates the influence of hydrophobic moiety incorporation in the polymer network. The addition of *t*-BMA clearly shifts the onset of pH-dependent swelling from ~7.4 to pH 7.0. Maximum volume swelling of these networks occurs near pH 6.0, characteristic of the early endosomes. Incorporation of t-BAEMA also lowers the onset of pH-dependent swelling, though the effect is less pronounced. The degree of volume swelling is decreased in PDETB30 and PDESSB30 relative to PDETB and PDETBA20 due to stronger hydrophobic associations in the polymer core and decreased ionizable amine content. Polymers crosslinked with TEGDMA and a degradable disulfide linker exhibit nearly identical swelling properties. All preparations exhibited a collapsed hydrodynamic diameter of 70 – 100 nm as determined by dynamic light scattering.

Measurements of the effective surface ζ-potential reveal insignificant difference between the various formulations. These data are consistent with the expectation that the PEG-grafted surface of these nanoscale hydrogels are very similar and that the modifications in chemical composition primarily affect the network core. All formulations posses a reversible surface charge, with an isoelectric point (IEP) at approximately pH 8.0, slightly positive ζ-potential at pH 7.4, and a maximum ζ-potential of 25 - 30 mV at pH 3.50. At physiological pH, the slightly positive ζ-potential may help facilitate non-specific cell-uptake. The negative ζ-potential observed from pH 10.5 to ~ pH 8.0 can be ascribed to the adsorption of negatively charged hydroxyl ions on the PEG-coated surface [68]. Likewise, the positive ζ-potential can be ascribed the surface adsorption of hydronium ions and protonation of amine-containing groups in the network core.

Hemolysis experiments were used to evaluate the ability of these hydrogels to disrupt erythrocyte membranes as a measure of their endosomolytic ability. These data (not shown) suggest these nanogels have utility in intracellular delivery applications as polymers mediate erythrocyte membrane disruption in a concentration- and pH-dependent manner. At pH 6.50, PDETB20 demonstrates excellent hemolytic ability, lysing over 80% of erythrocytes at 1 μg $mL^{-1}$ and nearly 100% at 100 μg $mL^{-1}$. These data, coupled with cytotoxicity results, indicate these nanoscale hydrogels are promising agents for delivery of biomacromolecules.

The effect of polymer concentration and composition on cellular proliferation was assessed using an MTS assay. As seen in Figure 10, PDETB15 and PDETB20 are non-toxic to Caco-2 cells at concentrations below 0.5 mg $mL^{-1}$. From 0.05 mg $mL^{-1}$ – 2 mg $mL^{-1}$, these formulations are significantly less toxic than the base formulation of P(DEAEMA-*g*-PEG) (PDET). It has been well documented that free amino groups contribute to the untoward cytotoxicity of many polycationic delivery agents and that increased cationic charge density correlates with increased cytotoxicity [69]. As expected, polymers with similar cationic charge densities, e.g. nanogels with 15 mol% and 20 mol% t-BAEMA and PDET, exhibit similar toxicity profiles. By nature of the polymer composition, nanogels with 15 mol% and 20 mol% t- BMA have less cationic charge density and thus result in decreased toxicity.

## CONCLUSION

We have synthesized novel pH-responsive hydrogel materials with diverse length scales and physicochemical properties. Because of their pH-dependent conformational change, these materials can protect entrapped therapeutics in their collapsed state and permit diffusion of solvent and drug in the swollen state. The ability to load and release insulin in P(MAA-g-EG) hydrogels can be modulated by the chemical nature and molecular weight of bioadhesion-promoting polysaccharides, including dextran and pullulan. Interpenetrating networks of P(MAA-g-EG) and P(BA) demonstrated controlled release of the model drug flourescein over four hours. Physicochemical properties, including particle size, volume swelling ratio, and critical swelling pH, of nanoscale hydrogels P(MAA-co-*t*-BMA-g-PEG), P(DEAEMA-co-t-BMA-g-PEG), and P(DEAEMA-co-t-BAEMA-g-PEG), were investigated using electron microscopy and dynamic light scattering. These properties can be modulated by tuning the polymer composition. Incorporation of hydrophobic moieties into the polymer core of P(DEAEMA-g-PEG) serves to lower the critical swelling pH while concomitantly decreasing cytotoxicity by decreasing cationic charge density. Nanogels synthesized with t-BMA exhibit favorable pH-responsive behavior for intracellular delivery and offer an excellent cytocompatibility. Our results suggest these novel hydrogel networks have great potential for transmucosal and intracellular delivery of proteins, chemotherapeutics, and siRNA.

## Acknowledgments

This work was supported grants from the National Institutes of Health (No. EB-00246-18), the NIH/NCI Center for Oncophysics (CTO PSOC U54-CA-143837), and the National Science Foundation (No. 1033746). W.B.L. and C.A.S. acknowledge the National Science Foundation for Graduate Research Fellowships. M.A.P. acknowledges the National Science Foundation for an NSF-IGERT fellowship.

## IV. REFERENCES

1. Peppas NA, Bures P, Leobandung W, Ichikawa H. Hydrogels in pharmaceutical formulations. European Journal of Pharmaceutics and Biopharmaceutics. 2000; 50(1):27–46. [PubMed: 10840191]
2. Wood KM, Stone GM, Peppas NA. Wheat germ agglutinin functionalized complexation hydrogels for oral insulin delivery. Biomacromolecules. 2008; 9(4):1293–1298. [PubMed: 18330990]
3. Fisher O, Kim T, Dietz S, Peppas N. Enhanced Core Hydrophobicity, Functionalization and Cell Penetration of Polybasic Nanomatrices. Pharmaceutical Research. 2009; 26(1):51–60. [PubMed: 18751960]
4. Wood KM, Stone GM, Peppas NA. The effect of complexation hydrogels on insulin transport in intestinal epithelial cell models. Acta Biomaterialia. 2010; 6(1):48–56. [PubMed: 19481619]
5. Betancourt T, Pardo J, Soo K, Peppas NA. Characterization of pH-responsive hydrogels of poly(itaconic acid-g-ethylene glycol) prepared by UV-initiated free radical polymerization as biomaterials for oral delivery of bioactive agents. Journal of Biomedical Materials Research Part A. 2010; 93A(1):175–188. [PubMed: 19536838]
6. Liechty WB, Kryscio DR, Slaughter BV, Peppas NA. Polymers for Drug Delivery Systems. Annual Review of Chemical and Biomolecular Engineering. 2010; 11:149–173.
7. Liechty WB, Peppas NA. Synthesis and In Vitro Characterization of pH-Responsive Nanogels for Oral Delivery of siRNA. Proceed Intern Symp Polym Therap. 2010; 8:71.
8. Serra L, Doménech J, Peppas NA. Design of poly(ethylene glycol)-tethered copolymers as novel mucoadhesive drug delivery systems. European Journal of Pharmaceutics and Biopharmaceutics. 2006; 63(1):11–18. [PubMed: 16368228]
9. Phillips MA, Peppas NA. Hydrogels modified with carbohydrates for oral protein delivery. Trans Ann Biomater Meeting. 2009; 33:267.

10. Lowman AM, Morishita M, Kajita M, Nagai T, Peppas NA. Oral delivery of insulin using pH-responsive complexation gels. Journal of Pharmaceutical Sciences. 1999; 88(9):933–937. [PubMed: 10479357]
11. Torres-Lugo M, Peppas NA. Molecular Design and in vitro Studies of Novel pH-Sensitive Hydrogels for the Oral Delivery of Calcitonin. Macromolecules. 1999; 32:6646–6651.
12. Kamei N, Morishita M, Chiba H, Kavimandan NJ, Peppas NA, Takayama K. Complexation hydrogels for intestinal delivery of interferon [beta] and calcitonin. Journal of Controlled Release. 2009; 134(2):98–102. [PubMed: 19095021]
13. Huang YB, Leobandung W, Foss A, Peppas NA. Molecular aspects of muco- and bioadhesion: Tethered structures and site-specific surfaces. Journal of Controlled Release. 2000; 65(1–2):63–71. [PubMed: 10699271]
14. Huang YB, Szleifer I, Peppas NA. Gel-gel adhesion by tethered polymers. Journal of Chemical Physics. 2001; 114(8):3809–3816.
15. Peppas NA, Huang YB. Nanoscale technology of mucoadhesive interactions. Advanced Drug Delivery Reviews. 2004; 56(11):1675–1687. [PubMed: 15350296]
16. Peppas NA. Molecular design and cellular response of novel intelligent mucoadhesive carriers for oral delivery of proteins. Architecture and Application of Biomaterials and Biomolecular Materials. 2004; 1:381–392. 465.
17. Thomas, B.; Tingsanchali, JH.; Creecy, CM.; Rosales, AM.; McGinity, JW.; Peppas, NA. Advances in Medical Engineering. Peppas, ASHNA.; Kanamori, T.; Tojo, K., editors. AIChE; New York: 2006. p. 249-254.
18. Peppas NA, Thomas JB, McGinty J. Molecular Aspects of Mucoadhesive Carrier Development for Drug Delivery and Improved Absorption. Journal of Biomaterials Science-Polymer Edition. 2009; 20(1):1–20. [PubMed: 19105897]
19. Lowman AM, Peppas NA. Molecular analysis of interpolymer complexation in graft copolymer networks. Polymer. 2000; 41(1):73–80.
20. Lowman, AM.; Peppas, NA.; Morishita, M.; Nagai, T. Tailored Polymeric Materials for Controlled Delivery Systems. McCulloch, I.; Shalaby, SW., editors. Vol. 709. ACS; Washington, D.C: 1999. p. 156-164.
21. Lowman AM, Peppas NA. Solute Transport Analysis in pH-Responsive, Complexing Hydrogels of Poly(Methacrylic Acid-g-Ethylene Glycol). Journal Of Biomaterials Science-Polymer Edition. 1999; 10:999–1009. [PubMed: 10574613]
22. Lowman, AM.; Peppas, NA. ACS Symposium Series. Dinh, SM.; DeNuzzio, JD.; Comfort, AR., editors. Vol. 728. ACS; Washington, D.C: 1999. p. 30-42.
23. Mathiowitz E, Jacob JS, Jong YS, Carino GP, Chickering DE, Chaturvedi P, Santos CA, Vijayaraghavan K, Montgomery S, Bassett M, Morrell C. Biologically erodable microsphere as potential oral drug delivery system. Nature. 1997; 386(6623):410–414. [PubMed: 9121559]
24. Morishita M, Peppas NA. Is the oral route possible for peptide and protein drug delivery? Drug Discovery Today. 2006; 11(19–20):905–910. [PubMed: 16997140]
25. Roberts RL, Sandra A. Receptor-Mediated Endocytosis of Insulin by Cultured Endothelial-Cells. Tissue & Cell. 1992; 24(5):603–611. [PubMed: 1440582]
26. Yamagata T, Morishita M, Kavimandan NJ, Nakamura K, Fukuoka Y, Takayama K, Peppas NA. Characterization of insulin protection properties of complexation hydrogels in gastric and intestinal enzyme fluids. Journal of Controlled Release. 2006; 112(3):343–349. [PubMed: 16631271]
27. Peppas NA, Hilt JZ, Khademhosseini A, Langer R. Hydrogels in Biology and Medicine: From Molecular Principles to Bionanotechnology. Advanced Materials. 2006; 18(11):1345–1360.
28. Madsen F, Peppas NA. Complexation graft copolymer networks: swelling properties, calcium binding and proteolytic enzyme inhibition. Biomaterials. 1999; 20(18):1701–1708. [PubMed: 10503971]
29. Lehr CM. From sticky stuff to sweet receptors - Achievements, limits and novel approaches to bioadhesion. European Journal of Drug Metabolism and Pharmacokinetics. 1996; 21(2):139–148. [PubMed: 8839687]

30. Lehr CM. Bioadhesion Technologies for the Delivery of Peptide and Protein Drugs to the Gastrointestinal-Tract. Critical Reviews in Therapeutic Drug Carrier Systems. 1994; 11(2–3):119–160. [PubMed: 7600586]

31. Serra L, Domenech J, Peppas NA. Engineering design and molecular dynamics of mucoadhesive drug delivery systems as targeting agents. European Journal of Pharmaceutics and Biopharmaceutics. 2009; 71(3):519–528. [PubMed: 18976706]

32. Serra L, Domenech J, Peppas NA. Drug transport mechanisms and release kinetics from molecularly designed poly(acrylic acid-g-ethylene glycol) hydrogels. Biomaterials. 2006; 27(31): 5440–5451. [PubMed: 16828864]

33. Thomas JB, Creecy CM, McGinity JW, Peppas NA. Synthesis and properties of lightly crosslinked poly((meth)acrylic acid) microparticles prepared by free radical precipitation polymerization. Polymer Bulletin. 2006; 57(1):11–20.

34. Thomas JB, Tingsanchali JH, Rosales AM, Creecy CM, McGinity JW, Peppas NA. Dynamics of poly(ethylene glycol)-tethered, pH responsive networks. Polymer. 2007; 48(17):5042–5048. [PubMed: 18690288]

35. Morishita M, Goto T, Peppas NA, Joseph JI, Torjman MC, Munsick C, Nakamura K, Yamagata T, Takayama K, Lowman AM. Mucosal insulin delivery systems based on complexation polymer hydrogels: effect of particle size on insulin enteral absorption. Journal of Controlled Release. 2004; 97(1):115–124. [PubMed: 15147809]

36. Goto T, Morishita M, Kavimandan NJ, Takayama K, Peppas NA. Gastrointestinal transit and mucoadhesive characteristics of complexation hydrogels in rats. Journal Of Pharmaceutical Sciences. 2006; 95(2):462–469. [PubMed: 16381013]

37. Fisher OZ, Peppas NA. Polybasic Nanomatrices Prepared by UV-Initiated Photopolymerization. Macromolecules. 2009; 42(9):3391–3398. [PubMed: 20526378]

38. Marek SR, Conn CA, Peppas NA. Cationic nanogels based on diethylaminoethyl methacrylate. Polymer. 2010; 51(6):1237–1243. [PubMed: 20436948]

39. Owens DE, Jian Y, Fang JE, Slaughter BV, Chen YH, Peppas NA. Thermally Responsive Swelling Properties of Polyacrylamide/Poly(acrylic acid) Interpenetrating Polymer Network Nanoparticles. Macromolecules. 2007; 40(20):7306–7310.

40. Chari RVJ. Targeted delivery of chemotherapeutics: tumor-activated prodrug therapy. Advanced Drug Delivery Reviews. 1998; 31(1–2):89–104. [PubMed: 10837619]

41. Caldorera-Moore M, Peppas NA. Micro- and nanotechnologies for intelligent and responsive biomaterial-based medical systems. Advanced Drug Delivery Reviews. 2009; 61(15):1391–1401. [PubMed: 19758574]

42. Caldorera-Moore M, Guimard N, Shi L, Roy K. Designer nanoparticles: incorporating size, shape and triggered release into nanoscale drug carriers. Expert Opinion on Drug Delivery. 2010; 7(4): 479–495. [PubMed: 20331355]

43. Brannon-Peppas L, Blanchette JO. Nanoparticle and targeted systems for cancer therapy. Advanced Drug Delivery Reviews. 2004; 56(11):1649–1659. [PubMed: 15350294]

44. Sparreboom A, de Jonge MJA, Verweij J. The use of oral cytotoxic and cytostatic drugs in cancer treatment. European Journal of Cancer. 2002; 38(1):18–22. [PubMed: 11750835]

45. Liu G, Franssen E, Fitch M, Warner E. Patient preferences for oral versus intravenous palliative chemotherapy. Journal of Clinical Oncology. 1997; 15(1):110–115. [PubMed: 8996131]

46. Kanard A, Jatoi A, Castillo R, Geyer S, Schulz TK, Fitch TR, Rowland KM, Nair S, Krook JE, Kugler JW. Oral vinorelbine for the treatment of metastatic non-small cell lung cancer in elderly patients: a phase II trial of efficacy and toxicity. Lung Cancer. 2004; 43(3):345–353. [PubMed: 15165094]

47. Hoff PM, Ansari R, Batist G, Cox J, Kocha W, Kuperminc M, Maroun J, Walde D, Weaver C, Harrison E, Burger HU, Osterwalder B, Wong AO, Wong R. Comparison of Oral Capecitabine Versus Intravenous Fluorouracil Plus Leucovorin as First-Line Treatment in 605 Patients With Metastatic Colorectal Cancer: Results of a Randomized Phase III Study. Journal of Clinical Oncology. 2001; 19(8):2282–2292. [PubMed: 11304782]

48. Van Cutsem E, Twelves C, Cassidy J, Allman D, Bajetta E, Boyer M, Bugat R, Findlay M, Frings S, Jahn M, McKendrick J, Osterwalder B, Perez-Manga G, Rosso R, Rougier P, Schmiegel WH,

Seitz JF, Thompson P, Vieitez JM, Weitzel C, Harper P. Oral Capecitabine Compared With Intravenous Fluorouracil Plus Leucovorin in Patients With Metastatic Colorectal Cancer: Results of a Large Phase III Study. Journal of Clinical Oncology. 2001; 19(21):4097–4106. [PubMed: 11689577]

49. Polizzi D, Pratesi G, Monestiroli S, Tortoreto M, Zunino F, Bombardelli E, Riva A, Morazzoni P, Colombo T, Dâ€™Incalci M, Zucchetti M. Oral Efficacy and Bioavailability of a Novel Taxane. Clinical Cancer Research. 2000; 6(5):2070–2074. [PubMed: 10815934]
50. Pescovitz MD, Rabkin J, Merion RM, Paya CV, Pirsch J, Freeman RB, O'Grady J, Robinson C, To Z, Wren K, Banken L, Buhles W, Brown F. Valganciclovir Results in Improved Oral Absorption of Ganciclovir in Liver Transplant Recipients. Antimicrob Agents Chemother. 2000; 44(10):2811–2815. [PubMed: 10991864]
51. O'Neill VJ, Twelves CJ. Oral cancer treatment: developments in chemotherapy and beyond. Br J Cancer. 2002; 87(9):933–937. [PubMed: 12434279]
52. Peppas NA, Wood KM, Blanchette JO. Hydrogels for oral delivery of therapeutic proteins. Expert Opinion on Biological Therapy. 2004; 4(6):881–887. [PubMed: 15174970]
53. Blanchette J, Kavimandan N, Peppas NA. Principles of transmucosal delivery of therapeutic agents. Biomedecine & Pharmacotherapy. 2004; 58(3):142–151.
54. Blanchette J, Peppas NA. Oral Chemotherapeutic Delivery: Design and Cellular Response. Annals of Biomedical Engineering. 2005; 33(2):142–149. [PubMed: 15771268]
55. Blanchette J, Peppas NA. Cellular evaluation of oral chemotherapy carriers. Journal of Biomedical Materials Research Part A. 2005; 72A(4):381–388. [PubMed: 15666363]
56. Owens DE, Eby JK, Jian Y, Peppas NA. Temperature-responsive polymer-gold nanocomposites as intelligent therapeutic systems. Journal of Biomedical Materials Research Part A. 2007; 83A(3):692–695. [PubMed: 17530631]
57. Fire A, Xu S, Montgomery MK, Kostas SA, Driver SE, Mello CC. Potent and specific genetic interference by double-stranded RNA in Caenorhabditis elegans. Nature. 1998; 391(6669):806. [PubMed: 9486653]
58. Whitehead KA, Langer R, Anderson DG. Knocking down barriers: advances in siRNA delivery. Nature Reviews Drug Discovery. 2009; 8(2):129–138.
59. Tamura A, Oishi M, Nagasaki Y. Enhanced Cytoplasmic Delivery of siRNA Using a Stabilized Polyion Complex Based on PEGylated Nanogels with a Cross-Linked Polyamine Structure. Biomacromolecules. 2009; 10(7):1818–1827. [PubMed: 19505137]
60. Convertine AJ, Benoit DSW, Duvall CL, Hoffman AS, Stayton PS. Development of a novel endosomolytic diblock copolymer for siRNA delivery. Journal of Controlled Release. 2009; 133(3):221–229. [PubMed: 18973780]
61. Bauhuber S, Hozsa C, Breunig M, Gopferich A. Delivery of Nucleic Acids via Disulfide-Based Carrier Systems. Advanced Materials. 2009; 21(32–33):3286–3306. [PubMed: 20882498]
62. van Dijk-Wolthuis WNE, Franssen O, Talsma H, van Steenbergen MJ, Kettenes-van den Bosch JJ, Hennink WE. Synthesis, Characterization, and Polymerization of Glycidyl Methacrylate Derivatized Dextran. Macromolecules. 1995; 28(18):6317–6322.
63. Gao H, Tsarevsky NV, Matyjaszewski K. Synthesis of Degradable Miktoarm Star Copolymers via Atom Transfer Radical Polymerization. Macromolecules. 2005; 38(14):5995–6004.
64. Carr DA, Peppas NA. Assessment of poly(methacrylic acid-co-N-vinyl pyrrolidone) as a carrier for the oral delivery of therapeutic proteins using Caco-2 and HT29-MTX cell lines. Journal of Biomedical Materials Research Part A. 2010; 92A(2):504–512. [PubMed: 19213059]
65. Moriyama K, Yui N. Regulated insulin release from biodegradable dextran hydrogels containing poly(ethylene glycol). Journal of Controlled Release. 1996; 42(3):237–248.
66. Inomata H, Goto S, Saito S. Phase-Transition of N-Substituted Acrylamide Gels. Macromolecules. 1990; 23(22):4887–4888.
67. Schild HG. Poly (N-Isopropylacrylamide) - Experiment, Theory and Application. Progress in Polymer Science. 1992; 17(2):163–249.
68. Chan YHM, Schweiss R, Werner C, Grunze M. Electrokinetic Characterization of Oligo- and Poly(ethylene glycol)-Terminated Self-Assembled Monolayers on Gold and Glass Surfaces. Langmuir. 2003; 19(18):7380–7385.

69. Fischer D, Li YX, Ahlemeyer B, Krieglstein J, Kissel T. In vitro cytotoxicity testing of polycations: influence of polymer structure on cell viability and hemolysis. Biomaterials. 2003; 24(7):1121–1131. [PubMed: 12527253]

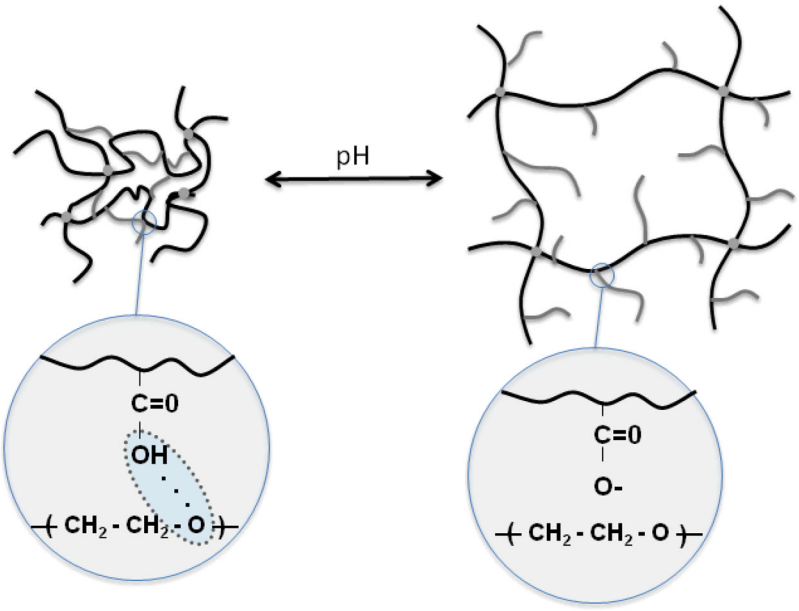


**Figure 1.**
Schematic of pH responsive hydrogels and the effect of complexation on the correlation length (pore size) ξ for pH responsive hydrogels

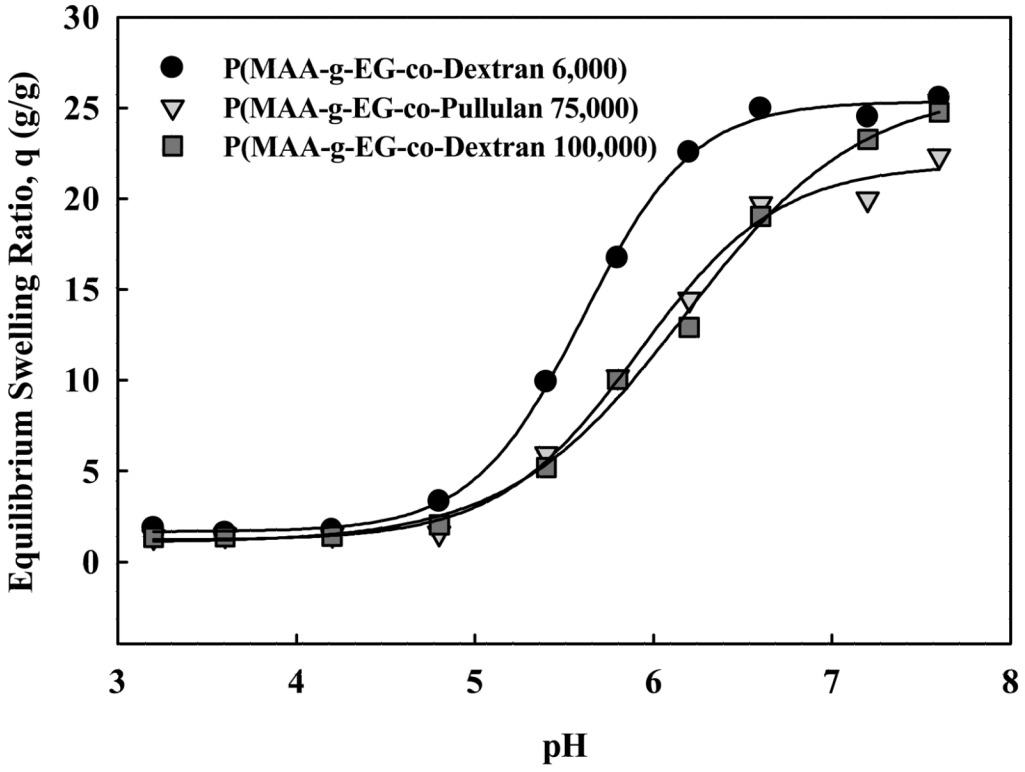


**Figure 2.**
pH-dependent equilibrium swelling of P(MAA-g-EG-Dextran 6000) (●), P(MAA-g-EG-Dextran 100000) (■), and P(MAA-g-EG-Pullulan 75000) (▼).

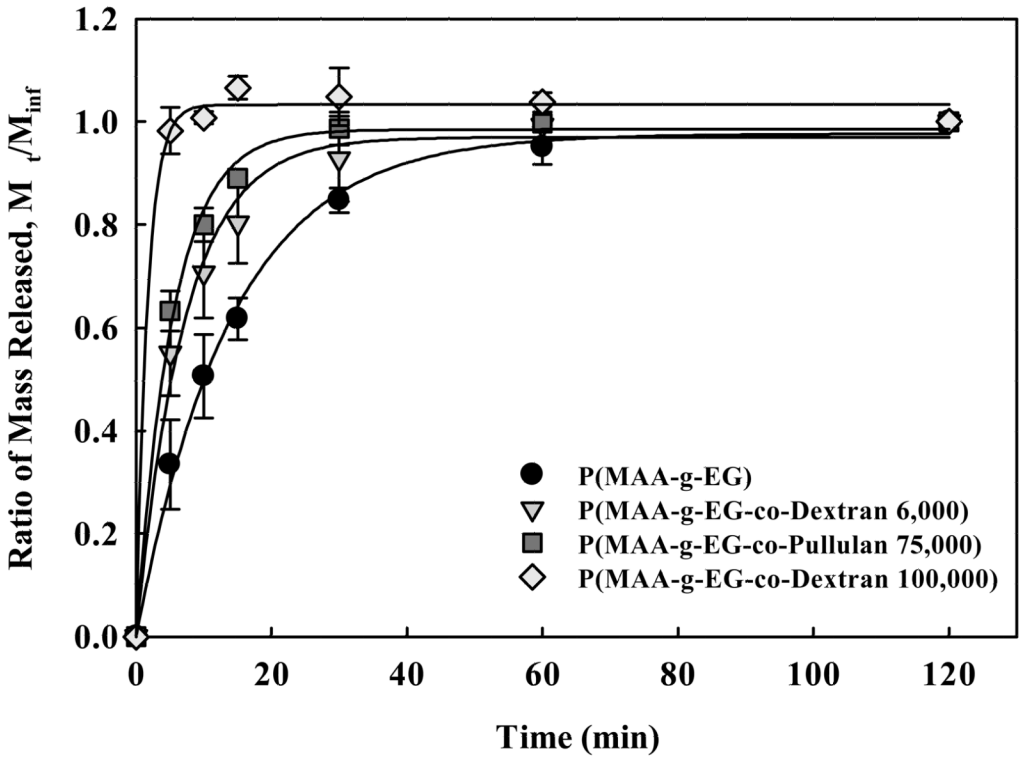


**Figure 3.**
Insulin release from microparticles of P(MAA-g-EG-Dextran 100,000) (◇), P(MAA-g-EG-Pullulan) (■), P(MAA-g-EG-Dextran 6,000) (▼), and P(MAA-g-EG) controls (●).

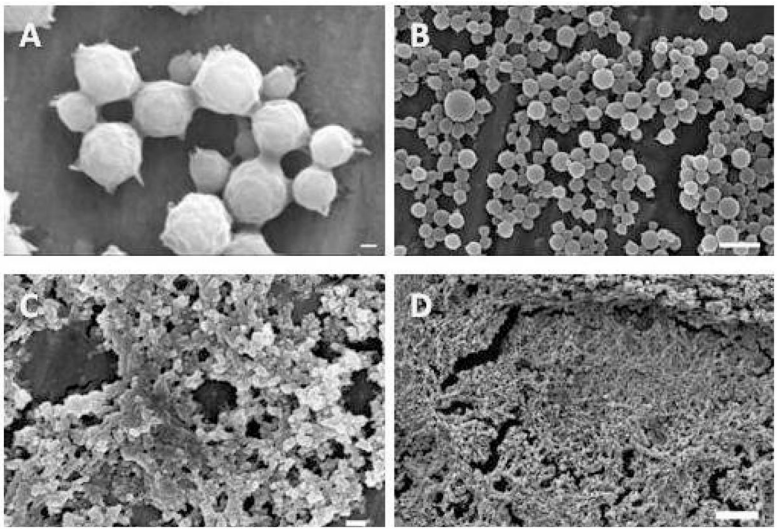


**Figure 4.**
Scanning electron microscopy of P(MAA-g-EG) with t-BMA particles: (A-B) particles after purification and (C-D) particles after freeze dry lyophilization. Scale bars equals 200 nm (A and C), 2 μm (B), and 1 μm (D).

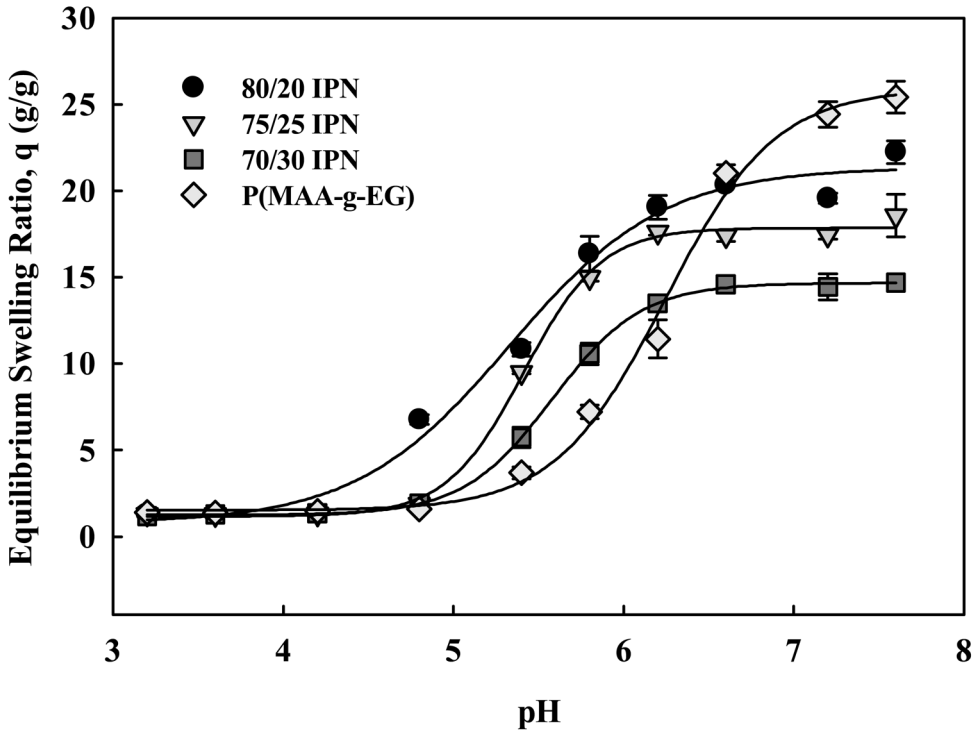


**Figure 5.**
pH-dependent equilibrium swelling of P(MAA-g-EG)/P(BA) IPN microparticles. 80/20 IPN (●), 75/25 IPN (▼), 70/30 IPN (■), and P(MAA-g-EG) (◇).

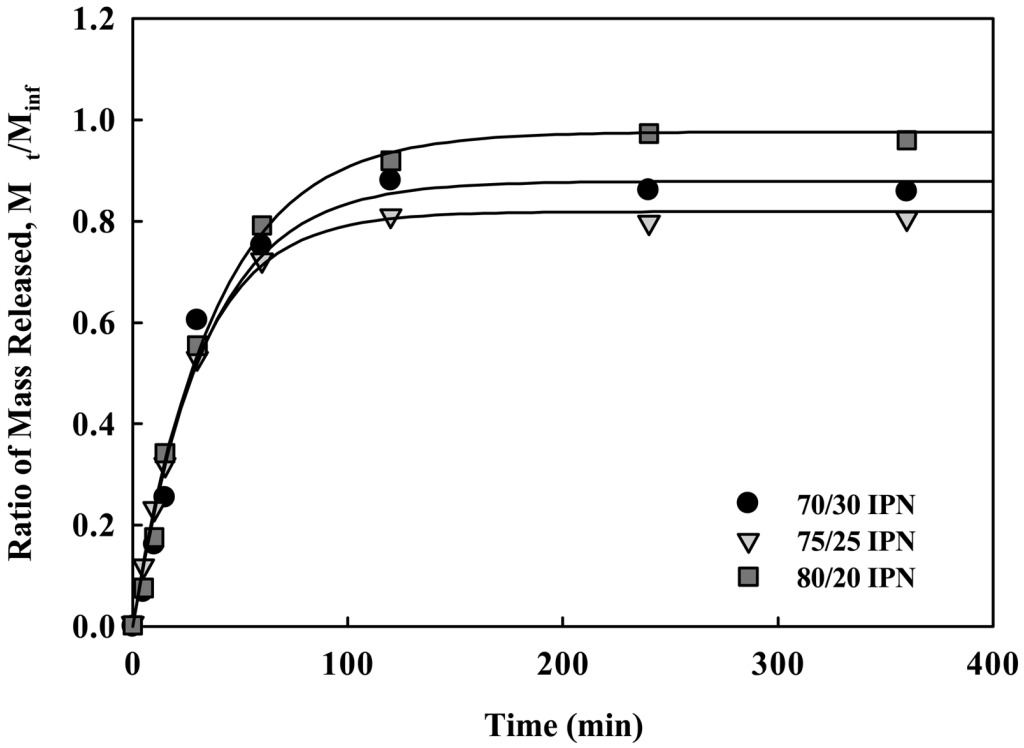


**Figure 6.**
Fluorescein release from crushed P(MAA-g-EG)/P(BA) IPN microparticles (75–500 μm) of 70/30 IPN (●), 75/25 IPN (▼), 80/20 IPN (■).

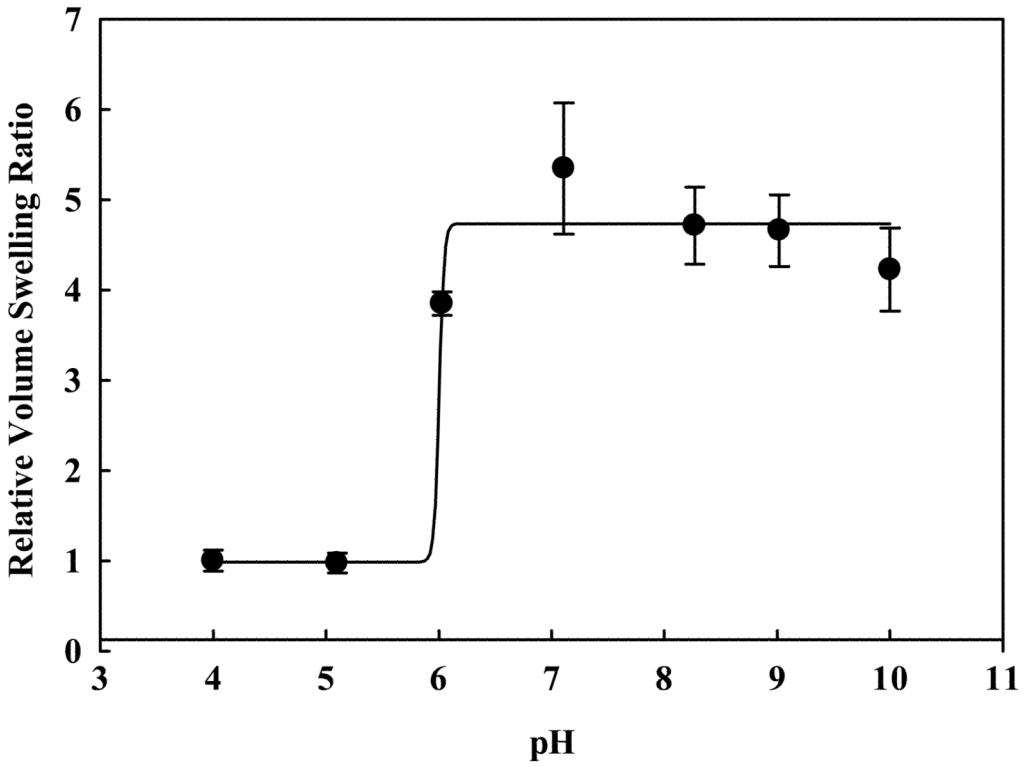


**Figure 7.**
Swelling profile of P(MAA-g-EG) with t-BMA nanoparticles as a function of pH.

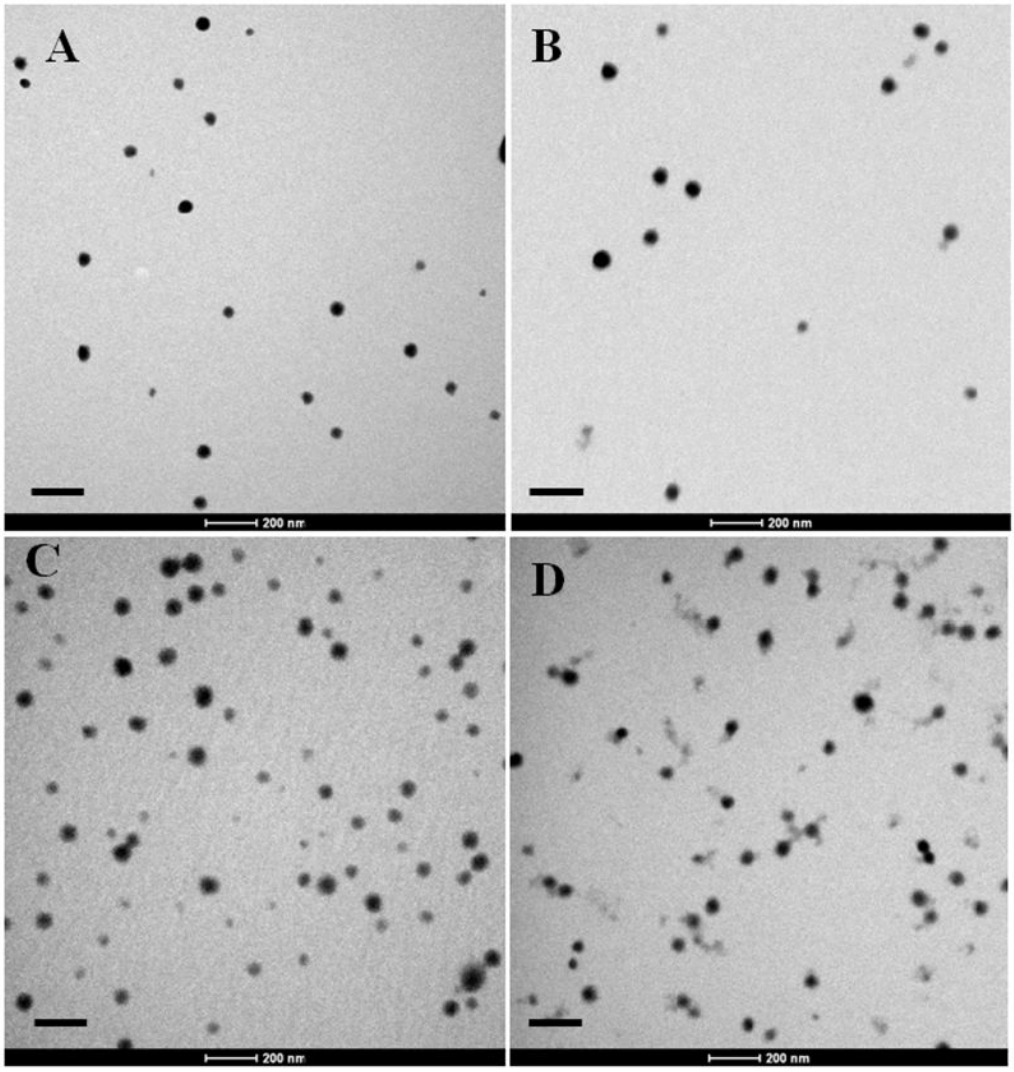


**Figure 8.**
Representative transmission electron microscopy images of TEGDMA-crosslinked P(DEAEMA-*g*-PEG) (A), TEGDMA-crosslinked P(DEAEMA-co-*t*-BAEMA-g-PEG) (B), TEGDMA-crosslinked P(DEAEMA-co-*t*-BMA-g-PEG) (C), and SSXL-crosslinked P(DEAEMA-co-*t*-BMA-g-PEG) (D). Particles stained with uranyl acetate and images collected at 43,000×. Scale bar represents 200 nm.

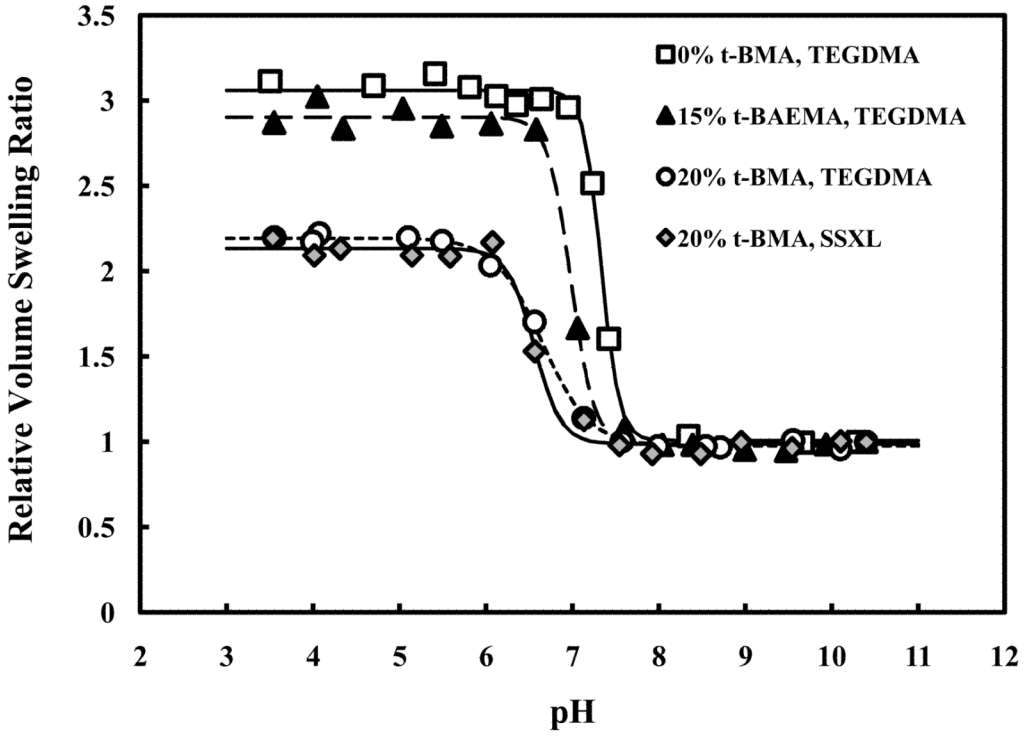


**Figure 9.**

pH-responsive behavior of nanogels in suspended in PBS. P(DEAEMA-*g*-PEG) (□), P(DEAEMA-co-*t*-BAEMA-g-PEG) crosslinked with tetra(ethylene glycol) dimethacrylate (▲), P(DEAEMA-co-*t*-BMA-g-PEG) crosslinked with tetra(ethylene glycol) dimethacrylate (○), and P(DEAEMA-co-*t*-BMA-g-PEG) crosslinked with bis(2-methacryloyloxyethyl) disulfide (◆).

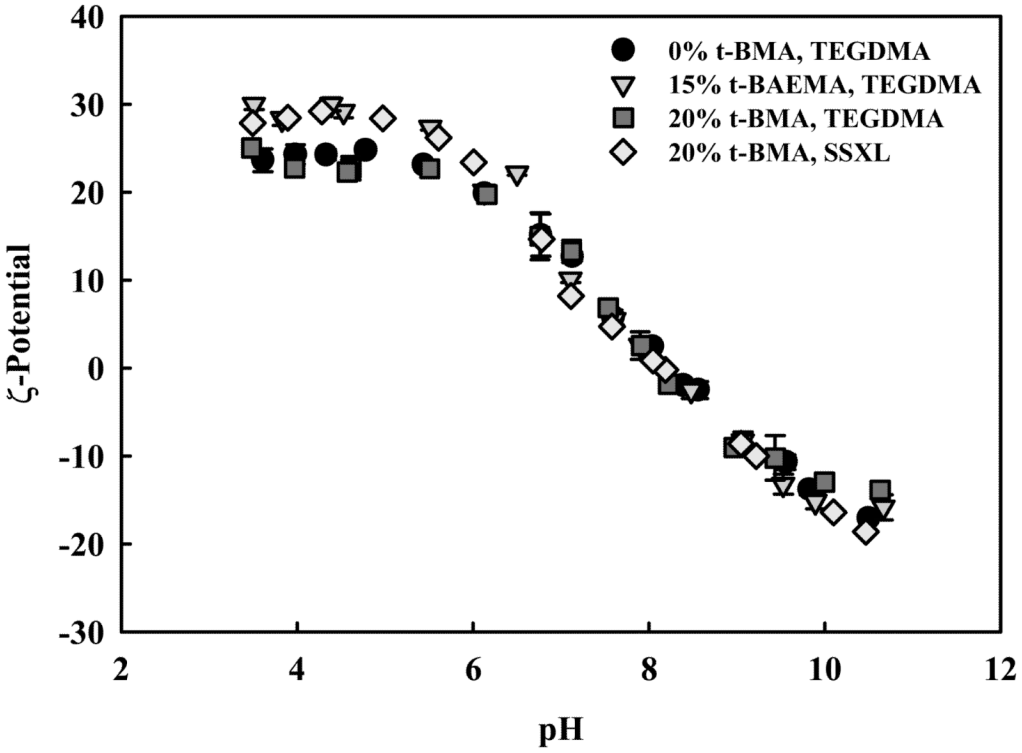


**Figure 10.**
Effective surface ζ-potential of various polymer formulations P(DEAEMA-*g*-PEG) (●), P(DEAEMA-co-*t*-BAEMA-g-PEG) crosslinked with tetra(ethylene glycol) dimethacrylate (▼), P(DEAEMA-co-*t*-BMA-g-PEG) crosslinked with tetra(ethylene glycol) dimethacrylate (■), and P(DEAEMA-co-*t*-BMA-g-PEG) cross linked with bis ( 2-methacryloyloxyethyl) disulfide (□). Data points represent the mean of 3 measurements ± SD.

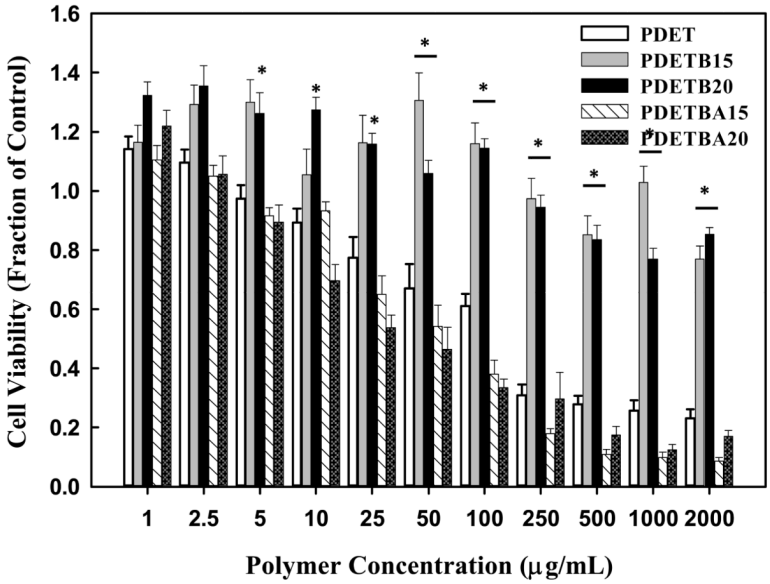


**Figure 11.**

Cytocompatibility of polycationic nanoscale hydrogels as a function of polymer concentration. The relative viability of Caco-2 cells was determined by MTS assay and is expressed as a fraction of the control (untreated) cells. Data are expressed as means ± SEM, n = 8. Statistical significance is noted relative to viability of cells exposed to PDET (* $p < 0.005$).

## Table 1

Comparison of contact angle measurements and loading efficiencies among P(MAA–g-EG)/P(BA) IPNs and P(MAA-g-EG) microparticles.

| Formulation | Contact Angle (°) | Loading Efficiency (%) |
|---|---|---|
| 80/20 IPN | 62 ± 1 | 25 ± 4 |
| 75/25 IPN | 68 ± 1 | 28 ± 3 |
| 70/30 IPN | 106 ± 1 | 45 ± 7 |
| P(MAA-g-EG) | 47 ± 1 | 21 ± 7 |